Carbon Capture, Utilization, and Storage from Power Plant Emissions

A Technical Report submitted to the Department of Chemical Engineering

Presented to the Faculty of the School of Engineering and Applied Science
University of Virginia • Charlottesville, Virginia

In Partial Fulfillment of the Requirements for the Degree
Bachelor of Science, School of Engineering

Cameron Lange
Spring, 2020

Technical Project Team Members
Rachel Berry
Abby Magner
Fiona Teevan-Kamhawi

On my honor as a University Student, I have neither given nor received unauthorized aid on this assignment as defined by the Honor Guidelines for Thesis-Related Assignments

Carbon Capture, Utilization, and Storage from Power Plant Emissions

Table of Contents:

Summary

The increased emission of carbon dioxide into the atmosphere from human activity, starting at the beginning of the Industrial Revolution, has proven to be the leading cause of climate change. Currently, massive efforts are being taken across the world to curb industrial carbon dioxide emissions using carbon storage and sequestration (CSS) technology. There are many environmental costs to current sequestration techniques.

This project attempts to analyze the feasibility of converting carbon dioxide captured from a natural gas power plant, Pastoria Energy Facility, into diesel. The plant is retrofitted with an amine scrubbing system to remove and isolate the carbon dioxide (CO_2) gas from the power plant exhaust using monoethanolamine (MEA). The CO_2 is then fed into a reverse water-gas shift reactor followed by a Fischer-Tropsch reactor, which converts the CO_2 into carbon monoxide (CO) and a variety of hydrocarbons, respectively.

The most profitable product produced by this process are C_{10}-C_{25} alkanes that will be sold as diesel fuel. The plant produces about 4500 kg of diesel per hour, or 10.7 million gallons per year, which is equivalent to 21.7 kg of diesel fuel produced per 1000 kg of CO_2 fed into the retrofitted process.

Due to economic factors, mainly concerning the cost of hydrogen fuel used throughout the reverse water-gas shift and Fischer-Tropsch reactions, it is recommended that the production of diesel fuel from CO_2 is not pursued and that the separated CO_2 should instead be stored in underground wells. The overall capital cost for this recommended option is $56,805,108 with utility costs of $26,392,029 per year, labor costs of $1,664,600 per year, and CO_2 transportation and storage costs of $6,411,006 per year. Overall, this project would remove 56,000 kg/hr of CO_2 from the atmosphere, a 27% reduction from the total plant emissions, at a process cost of

$34,804,505 per year. This cost for carbon removal can be offset by earned carbon credits of $6,740,000 per year and a price increase of 3.6% for 10 years and 3.0% after in electricity sold by the plant.

Introduction

As the world's population continues to grow exponentially, energy demands increase proportionally, and although renewable energy sources are becoming more prevalent, "fossil fuels [will] still account for more than three-quarters of world energy consumption through 2040" (Doman, 2017). Global CO_2 emissions, specifically those from burning fossil fuels, have risen exponentially over the past five years according to the World Resource Institute (Levin, 2018). The Environmental Protection Agency reports that about 27.5% of the CO_2 emitted in the US comes from electricity generation, and energy demand continues to rise rapidly. (United States Environmental Protection Agency, 2018), The International Energy Agency (IEA) reported a 2.3% increase in global energy demand in 2018, resulting in a 1.7% increase in CO_2 emissions from energy-related processes when compared to the prior year (Jungcurt, 2019). Energy-related CO_2 discharges from the United States alone amounted to 5,268 million metric tons in 2018 (IEA, 2019). Thus, while furthering the development of renewable fuels positively contributes to lessening society's reliance on fossil fuel-driven energy sources, action must be taken to reduce carbon dioxide emissions to provide an immediate, viable solution to the world's energy crisis. Carbon Capture, Utilization and Storage (CCUS) is a technology that enables the removal of carbon dioxide (CO_2) from gaseous emissions streams directly at their source, particularly at high-emissions facilities such as industrial power plants. While CCUS has been applied to pilot-scale operations, industries have yet to put forth the financial resources required to create large-scale systems. The primary challenge preventing this commitment is the drastic energy demand of separating carbon dioxide from other gases, resulting in a high cost. Based on initial CCUS designs, this single step alone "could consume 25 to 40% of the fuel energy of a power plant" (Haszeldine, 2009, p. 1648). In order for CCUS technology to thrive, design of the

separation process must be optimized to decrease its associated cost, which is the most pressing challenge and one of the primary objectives associated with the technical project.

The industrial site that will be used to model the CCUS process is the Pastoria Energy Facility (PEF), a 750 MW natural gas power plant near Bakersfield, California. This site was chosen due to the high concentration of CO_2 produced in the flue-gas exiting the stacks that are attached to the natural gas-fired turbines. In total, PEF generates approximately 1.5 billion kg of CO_2 per year. However, for the purpose of this project, a CCUS system will be modeled using only one of the facility's three existing stacks. Thus, our system will be receiving 510 million kg of CO_2 per year. The first step of separation involves cooling the flue-gas and feeding it to an absorption column, where it comes into contact with a solvent, which absorbs carbon dioxide, separating it from other gaseous compounds. The chosen solvent is monoethanolamine (MEA), C_2H_7NO, which will be composed of 30% MEA and 70% water by mass. The solvent stream exiting the absorber, which is rich in carbon dioxide, is heated and fed to a stripping column that separates the MEA from the desired carbon dioxide product (Liao et al., 2018, p. 528). In many of the previously executed applications of CCUS, the CO_2 is then liquified and stored underground or beneath the ocean floor. However, our goal is to transform the CO_2 into a diesel fuel product that can be used to power transportation. This will be accomplished through the Reverse Water-Gas Shift (RWGS) and Fischer-Tropsch (FT) reactions.

Previous Work

CCUS technologies are rapidly establishing their place in today's society. As of the year 2019, the International Energy Agency reports 30 million tons (Mt) of CO_2 emissions captured from 16 industrial-scale CCUS operating at facilities that produce fertilizer, steel, hydrogen, or process natural gas (IEA, 2019). The specific application of an amine scrubbing solvent composed of 30 wt% MEA to capture CO_2 from an industrial-scale facility was modeled by Monica Garcia, Hannah K. Knuutila, and Sai Gu, researchers in the Department of Chemical and Process Engineering at the University of Surrey and the Department of Chemical Engineering at the Norwegian University of Science and Technology, in 2017.

This research was utilized to guide decision-making in the design and operation of carbon separation equipment. This work developed simulations of absorption and desorption in ASPEN PLUS v8.6. Experimental data was compared to simulation results of absorption and resulted in good agreement after 78 experimental runs (Garcia, et al. 2017). Stripping column operation was validated through the use of four separate designs varying in diameter, packing height, and packing type, and compared to experimental data. Deviations were seen by Garcia, et al. in temperature of liquid flux exiting the stripper reboiler, and overall amount of CO_2 stripped depending on CO_2 loading in rich amine flux entering the stripper (2017).

The Reverse Water-Gas Shift reaction was discovered during the 19th century as a method of using carbon dioxide to produce water (Zubrin, 2018). Although CO_2 is a fairly unreactive molecule, it was discovered that through the addition of energy in the form of high temperatures, as well as maximizing the ratio of H_2 to CO_2, it is possible to create a thermodynamically favorable environment in which the conversion to CO and H_2O can occur (Pastor-Perez et al., 2017). In industrial applications, this reaction has been widely used in

conjunction with the Fischer-Tropsch reaction to convert syngas into a variety of hydrocarbon fuels.

The Fischer-Tropsch process was developed by Franz Fischer and Hans Tropsch, both chemists, in Germany in 1925 (Schulz, 1999). During World War II, it was used to synthesize replacement fuels for Germany because the country did not have access to petroleum (Schulz, 1999). Currently, it is only used at a small number of specialized chemical facilities to create long hydrocarbons from methane and/or syngas. There is a significant amount of research being done to synthesize fuels from a variety of carbon-based waste products, including municipal waste and biomass. Finland, as of 2019, is in the process of developing a Fischer-Tropsch process to convert biomass into fuels (VTT, 2019). This will be implemented in a paper mill where tree waste, like bark, will be processed into hydrocarbons to make fuel.

Audi's e-diesel project, which started in 2014, is still under development, as well. It intends to capture carbon dioxide from the atmosphere and convert it to diesel using the reverse water-gas shift reaction and the Fischer-Tropsch process and to use electrolysis to produce the necessary hydrogen (Audi, 2017). However, one of the biggest obstacles and controversies with this project is whether or not it is actually carbon neutral and cost effective. Electrolysis is expensive, especially on such a large scale, and requires the use of electricity, while hydrogen purchased from a methane reforming facility has a significant carbon footprint. Audi plans to use solar panels to get the necessary electricity for electrolysis, adding another element to the cost.

Process Flow Diagram

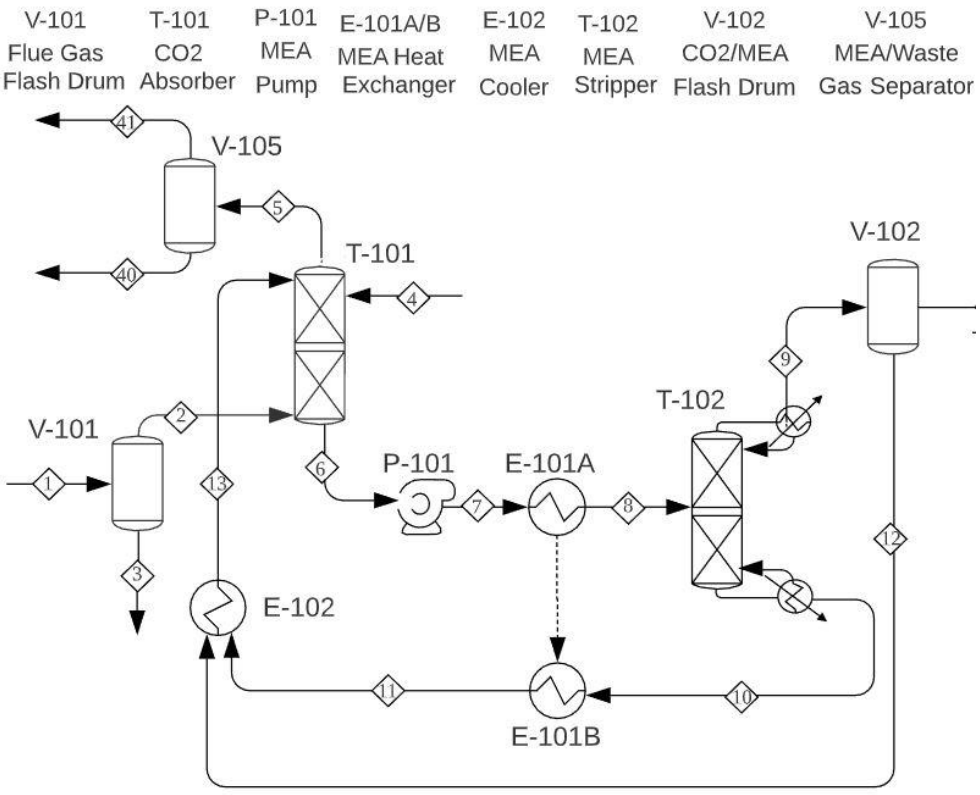

Figure 1: Process Flow Diagram: Amine Scrubbing

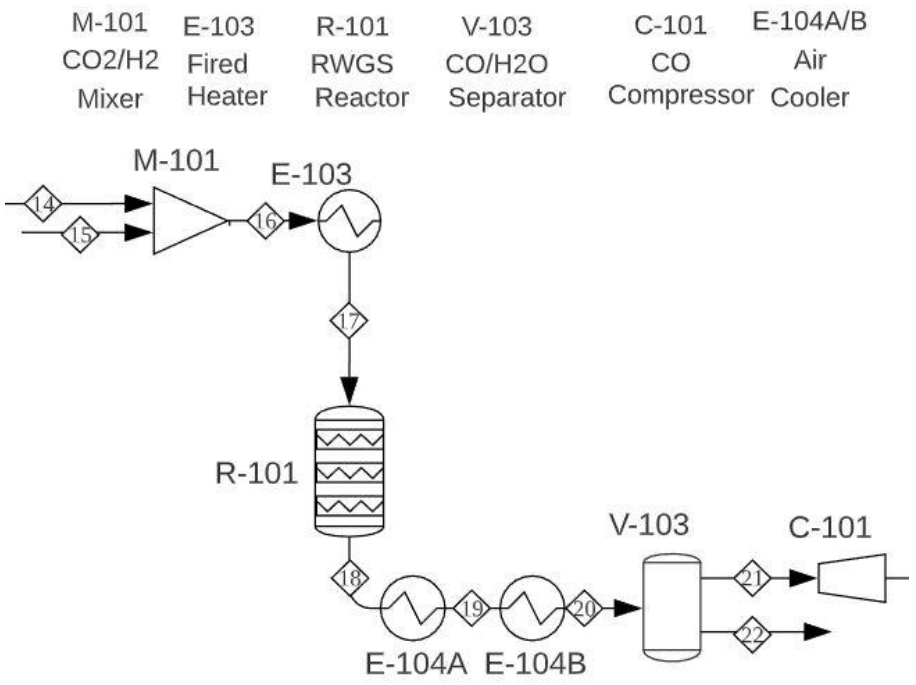

Figure 2: Process Flow Diagram - Reverse Water-Gas Shift Reaction

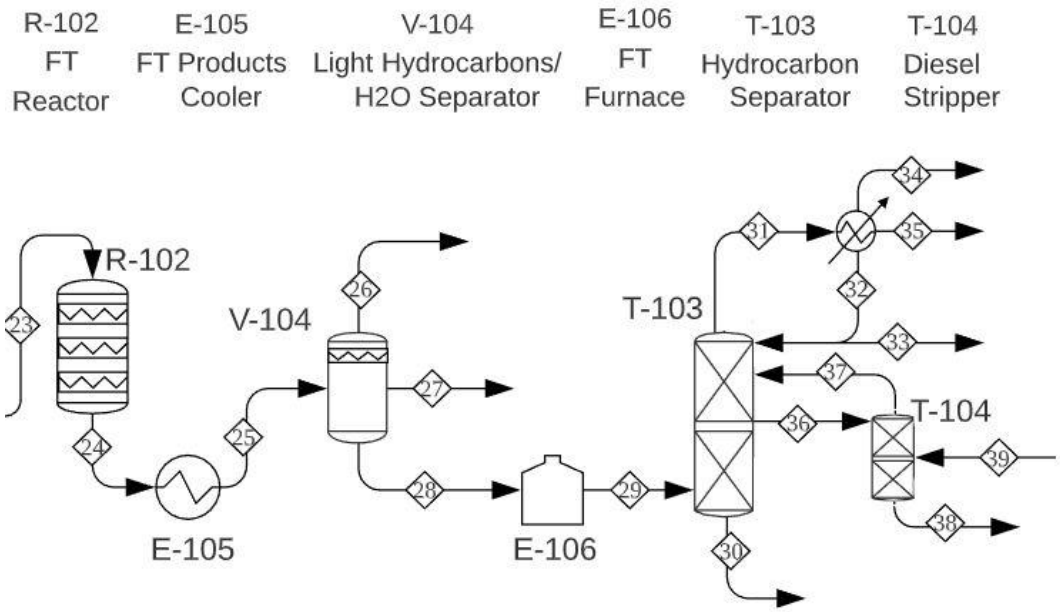

Figure 3: Process Flow Diagram - Fischer-Tropsch Reaction

Table 1: Absorption Stream Table

Stream Name	1	2	3	4	5	6	7	8
Description	Raw Flue Gas	Flue Gas	Wastewater	Lean MEA (Makeup)	Waste Gas	Rich MEA	Rich MEA	Hot Rich MEA
Temperature (°C)	150	40	40	40	64	49	49	130
Pressure (bar)	1.01	1.01	1.01	5.00	1.01	1.01	5.00	5.00
Mass Flow (metric ton/h)	478	435	42.6	27.9	411	571	571	571
Mole Flow (thousand kmol/h)	17.3	14.9	2.36	1.55	15.4	20.0	20.0	20.3
N_2 (kmol/h)	12,000	12,000	0.0223	0	12,000	0.0508	0.0508	0.0508
O_2 (kmol/h)	433	433	0.0015	0	433	0.0034	0.0030	0.0030
CO_2 (kmol/h)	1,560	1,560	0.126	0	280	0.472	0.472	313
H_2O (kmol/h)	3,290	928	2,360	1,550	2,700	16,600	16,600	16,600
MEA (kmol/h)	0	0	0	0.091	2.56	235	235	839
MEA^+ (kmol/h)	0	0	0	0	0	1,580	1,580	1,260
H_3O^+ (kmol/h)	0	0	0	0	0	0	0	0
$MEACOO^-$ (kmol/h)	0	0	0	0	0	1,490	1,490	1,200
HCO_3^- (kmol/h)	0	0	0	0	0	75.2	75.2	53.6
CO_3^{2-} (kmol/h)	0	0	0	0	0	6.37	6.37	0.943

Table 2: Stripping Stream Table

Stream Name	8	9	10	11	12	13	14
Description	Hot Lean MEA	Distillate	Bottoms (Lean MEA)	Cool Bottoms	H_2O recycle	Combined Recycle	CO_2 Stream
Temperature (°C)	130	111	152	51	45	40	45
Pressure (bar)	5	4	4	2	2	2	2
Mass Flow (metric ton/h)	571	69.5	502	502	12.7	515	56.7
Mole Flow (thousand kmol/h)	20.3	2.03	19.2	19.2	0.706	19.9	1.33
N_2 (kmol/h)	0.0508	0.0510	0	0	0	0	0.0510
O_2 (kmol/h)	0.00341	0.00341	0	0	0	0	0.00341
CO_2 (kmol/h)	313	1,260	0.613	0.000382	0.512	0.000152	1,260
H_2O (kmol/h)	16,600	771	15,900	15,900	706	16,600	65.1
MEA (kmol/h)	839	0.0151	2,690	2,690	0	2,680	0
MEA^+ (kmol/h)	1,260	0	310	315	0.0150	317	0
H_3O^+ (kmol/h)	0	0	0	0	0.000237	0	0
$MEACOO^-$ (kmol/h)	1,200	0	300	303	0	303	0
HCO_3^- (kmol/h)	53.6	0	9.64	2.17	0.0153	1.80	0
CO_3^{2-} (kmol/h)	0.943	0	0.284	4.70	0	6.43	0

Table 3: Overall Separation Process Stream Table

Stream Name	1	3	40	4	41	14
Description	Raw Flue Gas	Wastewater	MEA Recycle	Lean MEA (Makeup)	Waste Gas	CO_2 Stream
Temperature (°C)	150	40	64	40	64	45
Pressure (bar)	1.01	1.01	1.5	5	1.01	2
Mass Flow (metric ton/h)	478	42.6	4.99	27.9	411	56.7
Mole Flow (thousand kmol/h)	17.3	2.36	0.268	1.55	15.4	1.33
N_2 (kmol/h)	12,000	0.0223	0.00255	0	12,000	0.0510
O_2 (kmol/h)	433	0.00150	0.000164	0	433	0.00341
CO_2 (kmol/h)	1,560	0.126	0.00218	0	280	1,260
H_2O (kmol/h)	3,290	2,360	266	1,550	2,700	65.1
MEA (kmol/h)	0	0	0.577	0.091	2.56	0
MEA^+ (kmol/h)	0	0	1.13	0	0	0
H_3O^+ (kmol/h)	0	0	0	0	0	0
$MEACOO^-$ (kmol/h)	0	0	0.702	0	0	0
HCO_3^- (kmol/h)	0	0	0.385	0	0	0
CO_3^{2-} (kmol/h)	0	0	0.0217	0	0	0

Discussion of Design

Carbon Separation Equipment

The capture of CO_2 utilizing absorption is a proven commercially viable means to reduce environmental impact of greenhouse gas emissions at a point source. Amine scrubbing is a widely used technique for separation of CO_2 that has been around since the 1930's (Rochelle, 2009). This process is commonly separated into two stages: absorption and stripping. During absorption, flue gas from a power plant is directed into the bottom of a packed column and circulated countercurrently to the aqueous absorption solvent. The CO_2-rich solution is routed to a stripping column through a heat exchanger for high-temperature regeneration that reverses reactions that occurred between CO_2 and the solvent during absorption. Regenerated solvent is sent back to the absorber. Water vapor and gaseous CO_2 result and are sent to a condenser to obtain a rich CO_2 stream (Garcia, et al. 2017), which is then routed to the reverse water gas shift portion of the process.

ASPEN PLUS was utilized to predict process performance for design optimization of the absorption and stripping process. The ENRTL activity coefficient model was employed to ensure optimal modeling of electrolyte liquid phase nonidealities.

Typical flue gas from a natural gas-fired plant is composed of 2-3% O_2, 8-10% CO_2, 18-20% H_2O, and 67-72% N_2 by mole percent (Song, 2004). The Best Available Control Technology (BACT) utilized for regulation of NO_x emissions at the Pastoria Energy facility is XONON^{TM} control along with selective catalytic reduction (SCR) (Marjollet, 2016), so it can be assumed there is a negligible amount of NO_x and SO_x in the CCUS influent stream. This assumption is confirmed by data specific to the Pastoria Energy Facility gathered from the California Power Map reporting only 89.7 tons per year of NO_x emissions (Physicians,

Scientists, and Engineers for Healthy Energy, 2019). Emissions data for each major component of the flue gas after undergoing scrubbing is displayed in Table 1 below.

Table 4: Composition of Flue Gas Entering Absorber

Component	Mole %	Billion Moles Per Year	Mass Per Year Effluent (million metric tons)	Mass %	Mass Per Stack Per Year Effluent (million metric tons)	Mass per stack per hour (metric ton, assuming 7500 annual operational hours)
N_2	69.5	271	7.59	70.4%	2.53	336
O_2	2.5	9.74	0.312	2.9%	0.104	13.9
CO_2	9.0	35.1	1.54	14.3%	0.514	68.6
H_2O	19.0	74.0	1.33	12.4%	0.445	59.3

The CO_2 is separated from all other components in the flue gas through the use of a packed-bed absorption column loaded with an amine solvent with the ability to react selectively with CO_2 and regenerate under the correct stripper operation conditions. NO_x has the ability to slowly eat away at the amine solvent utilized during absorption, so it is imperative that scrubbing technology remains effective during the lifetime of the carbon separation equipment.

An amine solvent material must be chosen to balance biodegradability to protect the environment and stability at process conditions to ensure efficiency and safety. Sterically hindered amines, such as 2-amino-2-methylpropanol (AMP), are most stable at process conditions, but exhibit little to no biodegradability. Tertiary and cyclic amines also have very low biodegradability, and secondary amines, such as diethanolamine (DEA), 2-methylaminoethanol (MMEA), and N-(2-hydroxyethyl)-ethylenediamine (AEEA) provide highest process degradability (Eide-Haugmo, et al., 2011). Aqueous Monoethanolamine (MEA), a primary amine, is a well-researched and widely used material for CO_2 scrubbing at an industrial scale that is degradable under the correct conditions during wastewater treatment

(Eide-Haugmo, et al., 2011) and provides moderate stability at process conditions. This material was prioritized as the solvent of choice for the development of a carbon capture retrofit design for the Pastoria Energy facility.

MEA absorption of CO_2 includes chemistry involving CO_2 hydrolysis, water dissociation, carbamate hydrolysis, bicarbonate dissociation, and protonation of MEA (Zhang, 2013). Reactions for bicarbonate formation in going forward (1) and in reverse (2) are displayed below, and were gathered from Pinsent et al. (1956) The forward (3) and reverse (4) reactions for carbamate formation are retrieved from Hikita et al. (1997) and are also shown below. The forward reactions will occur in the absorber, while the reverse reactions ensue in the stripper promoted by heat and pressure.

$CO_2 + OH^- \rightarrow HCO_3^-$ (1)

$HCO_3^- \rightarrow CO_2 + OH^-$ (2)

$MEA + CO_2 + H_2O \rightarrow MEACOO^- + H_3O^+$ (3)

$MEACOO^- + H_3O^+ \rightarrow MEA + CO_2 + H_2O$ (4)

The forward (5) and reverse (6) kinetic expressions for bicarbonate formation (Pinsent et al., 1956), as well as carbamate formation forward (7) and reverse (8) kinetic expressions are as follows (Hikita et al., 1997). The symbol *i* represents an individual species, with K_i representing its chemical equilibrium and a_i as its activity. Individual reactions are represented by *j*, and their reaction rate is represented with k_j.

$$r_1 = k_8 * a_{CO_2} * a_{OH^-} \quad (5)$$

$$r_2 = \frac{k_8}{K_{HCO_3^-}} * a_{HCO_3^-} \quad (6)$$

$$r_3 = k_6 * a_{MEA} * a_{CO_2} \quad (7)$$

$$r_4 = \frac{k_6}{K_{MEACOO^-}} * \frac{a_{MEACOO^-} * a_{H_3O^+}}{a_{H_2O}} \quad (8)$$

The absorber is modeled with three theoretical stages, each at an equivalent packing height (HETP) of 3.33 meters for a total height of 10 meters and a diameter of 11.8 meters. The column is modeled packed with ½" ceramic berl saddles. The diameter of the column was provided by ASPEN given our constraints and operating parameters, and height was optimized through academic research and discussion with industry experts. Table 2 of "Review on the mass transfer performance of CO_2 absorption by amine-based solvents in low- and high-pressure absorption packed columns" provides examples of similarly functioning absorption columns operating optimally at packed heights ranging from 1.1-6.55 meters, with the majority of data centered at 3 meters (Afkhamipour, 2017). The column operates above atmospheric pressure, at 2 bar, to improve separation, decrease column size, and reduce compression requirements further downstream into the process. Specified operating parameters included temperature, pressure, height, number of theoretical stages, and feed stream location. Composition of distillate and bottoms streams, column diameter, pressure drop, and heat duty were obtained from simulations. Main goals included minimization of pressure drop across both the absorber and stripper and minimization of heat duty.

Review of literature suggested optimal equivalent packing heights for similarly modeled desorption columns ranging from 2.5-3.8 m (Garcia, et al. 2017). HETP for our system remained within this range until resulting parameters were optimized sufficiently. The stripper is modeled with eight theoretical stages, a total height of 17.1 m and a diameter of 13.4 m. The resulting HETP is 2.83 m. Inputs specified for the model were reflux ratio, bottoms rate, column height, number of stages, condenser and reboiler type, and feed stream location. The feed stream of rich MEA was modeled as a single-phase liquid solution. In actuality, it is possible that at high

loading the feed stream could flash prior to entering the stripping column. Resulting variances in enthalpy and CO_2 mass transfer from simulated results as well as temperatures higher than predicted would occur in this scenario (Garcia, et al. 2017). Simulation resulted in values for pressure drop, compositions of bottoms and distillate, column diameter, and heat duty.

Heat exchange equipment area was found through utilization of the heat exchanger design equation (9). The rate of heat transfer was given via ASPEN model of each piece of equipment, and the heat transfer coefficient was estimated using Appendix E: Heuristics for Process Equipment Design from Plant Design and Economics for Chemical Engineers, Fifth Edition (Anderson, n.d.). The log mean temperature difference was calculated using Equation 10.

$$Q = UA\Delta T_{lm} \quad (9)$$

$$\Delta T_{lm} = \frac{(T_{Hin} - T_{Cout}) - (T_{Hout} - T_{Cin})}{ln\frac{(T_{Hin} - T_{Cout})}{(T_{Hout} - T_{Cin})}} \quad (10)$$

Reverse Water Gas Shift Reaction

$$CO_2 + H_2 \rightarrow CO + H_2O \quad (11)$$

After the flue gas stream has passed through the absorption and stripping process, the resulting concentrated CO_2 stream is fed into the Reverse Water-Gas Shift (RWGS) reactor, a packed bed reactor containing 0.5 weight percent Ni/SiO_2 catalyst, which has a density of 6.97 g/cm^3. This catalyst was chosen because it provides preferable catalytic activity and high selectivity of CO (Wu et al., 2015, p. 4154). CO_2 reacts with pure hydrogen that will be purchased from a source outside of the overall process, which will likely be produced through solar-photovoltaic electrolysis. As shown by Reaction 1 above, the products of the RWGS reaction are CO and H_2O, and a 95% conversion of CO_2 was assumed. The reactor must operate at high temperatures in order for the catalytic reaction to occur, and a temperature of 400 ℃ was

chosen, which is on the lower end of previously studied ranges, while still allowing the desired conversion to be reached (Kumar et al., 2008, p. 4086). The rate expression that was chosen to model the kinetics of the RWGS reaction is the Langmuir-Hinshelwood model analyzed by Smith et al., where r is the rate of reaction in mol/cm^{3}s (2010).

$$r = \frac{kK_{CO}K_{H_2O}\left[P_{CO}P_{H_2O} - \frac{P_{CO_2}P_{H_2}}{K_{eq}}\right]}{(1+K_{CO}P_{CO} + K_{H_2O}P_{H_2O} + K_{CO_2}P_{CO_2})^2} \times \frac{\rho_{cat}}{60} \quad (12)$$

The equilibrium and rate constants are temperature-dependent, and were calculated according to the following expressions, where the rate constant, k, is in mol/(g-cat min).

$$K_{eq} = exp(\frac{4577.8}{T} - 4.33) \quad (13)$$

$$k = exp(\frac{-29364}{1.987 \times T} - \frac{40.32}{1.987}) \quad (14)$$

$$K_{CO} = exp(\frac{3064}{1.987 \times T} - \frac{6.74}{1.987}) \quad (15)$$

$$K_{H_2O} = exp(\frac{-6216}{1.987 \times T} + \frac{12.77}{1.987}) \quad (16)$$

$$K_{CO_2} = exp(\frac{12542}{1.987 \times T} - \frac{18.45}{1.987}) \quad (17)$$

The values of each constant are listed below in Table 5, which were calculated based on a temperature of 673 K.

Table 5: RWGS Rate and Equilibrium Constants

Constant	Value
K_{eq}	11.85
k (mol/(g-cat min))	0.19
KCO	0.33
KH_2O	5.92
KCO_2	1.10

These expressions were used in calculations performed in MATLAB to determine the amount of catalyst and reactor volume required for the RWGS reaction. The catalyst weight was calculated through the following integration:

$$W = F_{A,0} \int_0^X \frac{dX}{-r_A} \quad (18)$$

W represents the catalyst weight in grams, $F_{A,0}$ represents the initial molar flow rate of CO_2, X represents the conversion of CO_2, and r_A represents the rate expression listed above. It was determined that the required catalyst weight is 6.83 metric tons Ni/SiO_2. Dividing this value by the catalyst density gives a required reactor volume of 0.979 m^3. To determine the dimensions of the reactor, an aspect ratio of L/D = 4 was assumed. Based on the following equation,

$$V = \frac{1}{4}\pi D^3 \quad (19)$$

the diameter of the reactor is 0.678 meters, and the length is 2.712 m. These values were rounded up to a diameter of 1 meter and a length of 3 meters to eliminate additional costs associated with purchasing a custom sized reactor.

Having completed kinetics calculations in MATLAB, Aspen Plus was used to model the RWGS reactor and associated equipment. RK-SOAVE was chosen as the property method, and

the reaction was modeled using an RStoich block. This simulation produced the results displayed in Table 6 below. The pressure drop across the reactor was calculated using the Ergun equation,

$$\frac{\Delta p}{L} = \frac{150\mu(1-\varepsilon)^2 u_0}{\varepsilon^3 {d_p}^2} + \frac{1.75(1-\varepsilon)\rho {u_0}^2}{\varepsilon^3 d_p} \quad (20)$$

where $\Delta p$is the pressure drop in Pa, L is the length of the reactor in meters, $\mu$is the viscosity of the reaction mixture in Pa-s, ε is the catalyst void fraction, u_0 is the feed velocity in meters per second, d_p is the catalyst particle diameter in meters, and$\rho$is the density of the reaction mixture in kg/m^3. Based on physical property estimation in Aspen, μ and ρ were determined to be 0.264 millipoise and 0.449 kg/m^3, respectively. As shown in the calculation in the Appendix, this results in a pressure drop of 0.32 bar.

Table 6: RWGS Stream Table

Stream Name	14	15	16	17	18	19	20	21	22
Description	CO_2 Product	Pure H_2	Mixed CO_2/H_2	RWGS Feed	RWGS Product	E-104A Outlet	E-104B Outlet	Water Product	FT CO Feed
Temperature (°C)	45	45	45	400	400	200	40	40	40
Pressure (bar)	2	2	2	2	2	1.01	1.01	1.01	1.01
Mass Flow (metric ton/h)	57.4	7.73	57.4	65.2	65.2	65.2	65.2	42,100	46,200
Mole Flow (kmol/h)	1,330	3,830	1,330	5,180	5,180	5,180	5,180	1,050	4,130
H_2	0	3,830	0	3,830	2,620	2,620	2,620	0.000108	2,620
N_2	0.0510	0	0.0510	0.0510	0.0510	0.0510	0.0510	0	0.0510
O_2	0.00341	0	0.00341	0.00341	0.00341	0.00341	0.00341	0	0.00341
CO_2	1,260	0	1,260	1,260	63.9	63.9	63.9	0.000398	63.9
CO	0	0	0	0	1,210	1,210	1,210	1,210	1,210
H_2O	65.87	0	65.9	65.9	1,280	1,280	1,280	1,050	230
MEA	0	0	0	0	0	0	0	0	0

RWGS Heat Transfer & Auxiliary Equipment

E-103, a fired heater, is required to heat the RWGS feed stream from 45 ℃ to 400 ℃. The Aspen simulation of this heater indicates a heat duty of 16.9 MW. According to the PTW heuristics for fired heaters, the radiation rate is 38.0 kW/m^2, and the convection rate is 12.0 kW/m^2. These values were used to determine a required heat transfer area of 337 m^2.

E-104A/B is a series of two air coolers that bring the temperature of the R-101 product from 400 ℃ to 40 ℃. In the first step, E-104A cools the stream to 200 ℃, and the heat that is removed is used to generate steam that can be used when separating the Fischer-Tropsch products. The heat duty for E-104A is -9.04 MW. According to the heuristics provided in Turton for air coolers, the overall heat transfer coefficient, U, falls between 450-570 W/m^2℃. As shown in the calculation in the Appendix, this leads to a required heat transfer area of 88.6 m^2. Next, E-

104B cools the stream from 200 ℃ to 40 ℃. The heat duty for E-104B is -20.6 MW. This results in a heat transfer area of 252 m^2.

V-103 is a flash vessel that separates the products of the RWGS reaction into a wastewater stream and the carbon monoxide feed stream for the Fischer-Tropsch reaction. This piece of equipment operates at a temperature of 40 ℃ and a pressure of 1.01 bar. Based on sizing provided in the Aspen Economics section, the required vessel diameter is 3 meters, and the tangent to tangent height is 4 meters. The separator has a heat duty of 35.6 kW.

Fischer-Tropsch Synthesis

The Fischer-Tropsch synthesis converts carbon monoxide and hydrogen gas into hydrocarbons and water via the following reactions:

$$(2n+1)\,H_2 + nCO \rightarrow C_n\,H_{(2n+2)} + nH_2\,O \quad (21)$$

$$2nH_2 + nCO \rightarrow C_n\,H_{2n} + nH_2\,O \quad (22)$$

$$2nH_2 + nCO \rightarrow C_n\,H_{(2n+1)}\,OH + (n-1)H_2O \quad (23)$$

The reactions are exothermic with a heat of reaction of about -165 kJ/mol. Because alcohols make up a very small portion of the product, they were excluded from the Aspen simulation as a representative molecule. Alkanes with even carbon numbers were chosen to represent all C_n and C_{n+1} molecules. For example, C_2H_6 in Aspen represents C_2 and C_3 molecules.

The rate of carbon monoxide consumption via the Fischer-Tropsch synthesis using a cobalt catalyst is (Ostadi et al, 2016):

$$r_{CO} = (k{P_{CO}}^{0.65}\,{P_{H_2}}^{0.6})/(1 + K_1\ \ P_{CO}) \quad (25)$$

The constants at 220°C are K_1 = 41.30 MPa^{-1} and k = 0.6500 mol g_{cat}^{-1} h^{-1} $MPa^{-1.25}$ (Ostadi et al, 2016). The carbon monoxide kinetics were used to size the reactor using the mass of catalyst needed and the density of the catalyst which is 8.90 metric tons/m^3. The total volume required for 95% conversion was 17.1 m^3.. The inner diameter of the tubes was set to 38.1 mm (1.5 inches) as recommended for efficient heat transfer. The length of the tubes was set to 4.5 meters. Therefore, the number of tubes required is 3334. The pressure drop within the reactor tubes was found to be 0.7 bar. The reactor sizing, along with the product distribution, were determined using MATLAB.

Product distribution of the Fischer-Tropsch products are dependent on reactor temperature, pressure, and catalyst. The kinetics of the Fischer-Tropsch reaction are difficult to model using Aspen software but can be modelled using the Anderson-Schulz-Flory Distribution (ASF). ASF is used to estimate the product selectivity for a given probability of chain growth (Spath & Dayton, 2003):

$$W_n = n(1-\alpha)^2\alpha^{n-1} \quad (26)$$

W_n is the weight fraction of the component with n carbon atoms and α is the probability of chain formation. The approximate value for α for a cobalt catalyst in a reactor at 220 °C with a 2.15:1 ratio of H_2 to CO is 0.89. The rate equation above was used to find the yield for the reaction.

Aspen Plus was used to model the Fischer-Tropsch diesel synthesis as a whole. RStoic was used to model the reactor. A heat exchanger and a flash drum were used to bring the product stream down to 32 °C and 3.4 bar in order to separate the water and some of the lighter components from the desired hydrocarbons. The saturated steam generated from the heat exchanger is at and 10 barg and can be used to heat the reboiler. The distillation column was

modeled using RadFrac. The distillation column separates the gasoline components (usually C_5-C_{11}) from the diesel components (usually C_9-C_{25}) (Spath & Dayton, 2003) and the wax components (modeled as C_{30}) from gas and diesel. The wax components can be fed into a hydrocracking process in which the chains are broken up and diesel and gasoline are produced. However, this is out of the scope of this Capstone. Therefore, they will be burned to produce heat for the furnace E-106.

The condenser does not reach temperatures below 30 °C and has a cooling requirement of 3.42 MW. Cooling water at 20 °C will be used in this report to fulfill the cooling requirement.

Table 7: Table for R-102 product selectivity and yield

Carbon Number Representation	**Composition (wt%)**	**Calculated Selectivity (wt% hydrocarbons)**
C_1	Lighter Components Gasoline 30.3%	1.21%
C_2		5.03%
C_4		7.21%
C_6		8.26%
C_8		8.57%
C_{10}	Diesel 43.3%	8.18%
C_{12}		7.92%
C_{14}		7.27%
C_{16}		6.56%
C_{18}		5.82%
C_{20}		5.11%
C_{22}		4.44%
C_{24}	Waxes 26.3%	3.84%
C_{26}		3.29%
C_{28}		2.80%
C_{30+}		14.27%

Table 8: Reactor product and downstream operations stream tables

Stream	**23**	**25**	**27**	**26**
Description	**R-102 Product**	**V-104 Vapor**	**V-104 Hydrocarbon**	**V-104 Water**
Temperature (C)	220	60	60	60
Pressure (barg)	20	3.0	3.0	3.0
Mass Flow (kg/hr)	46200	7480	6530	32200
Mole Flow (kmol/hr)	1860	418	43.4	1395
H_2 (mole frac)	0.119	0.526	0	0
CO (mole frac)	0.0423	0.183	0.00113	0.00108
CH_4 (mole frac)	0.00672	0.0262	0.00121	0.00116
C_2 (mole frac)	0.0122	0.0396	0.00494	0.00471
CO_2 (mole frac)	0.0344	0.132	0.0110	0.00656
C_4 (mole frac)	0.00992	0.0145	0.00950	0.00904
C_6 (mole frac)	0.00794	0.0224	0.122	0
C_8 (mole frac)	0.00632	0.00583	0.213	0
C_{10} (mole frac)	0.00502	0	0.206	0
C_{12} (mole frac)	0.00399	0	0.169	0
C_{14} (mole frac)	0.00316	0	0.134	0
C_{16} (mole frac)	0.00251	0	0.107	0
C_{18} (mole frac)	0.00199	0	0.00269	0.00256
C_{20} (mole frac)	0.00158	0	0.00213	0.00203
C_{22} (mole frac)	0.00125	0	0.00169	0.00161
C_{24} (mole frac)	0	0	0.00160	0.00152
C_{26} (mole frac)	0	0	0.00106	0.00101
C_{28} (mole frac)	0	0	0.00101	0
C_{30} (mole frac)	0.00346	0	0.00467	0.00446
Water (mole frac)	0.735	0.0490	0.00494	0.964

Table 9: Stream table for the distillation outlets

Stream	**35**	**36**	**34**	**39**	**29**	**39**
Description	**Non-condensable**	**Water**	**Gasoline**	**Diesel**	**Wax**	**Stripping Steam**
Temperature (°C)	30	30	30	180.6	414.9	201.5
Pressure (bar)	1.71	1.71	1.71	1.71	1.71	16.01
Mass Flow (kg/hr)	7.07	181	1870	4502	148	180.2
Mole Flow (kmol/hr)	0.181	10.0	17.8	25.0	0.392	10.0
CO (mole frac)	0.186	0	0	0	0	0
CH_4 (mole frac)	0.0750	0	0.00219	0	0	0
C_2 (mole frac)	0.152	0	0.0105	0	0	0
CO_2 (mole frac)	0.476	0	0.0220	0	0	0
C_4 (mole frac)	0.0340	0	0.0228	0	0	0
C_6 (mole frac)	0.0441	0	0.0297	0	0.00316	0
C_8 (mole frac)	0.00794	0	0.517	0.00214	0.00757	0
C_{10} (mole frac)	0	0	0.124	0.270	0.0105	0
C_{12} (mole frac)	0	0	0	0.294	0.0120	0
C_{14} (mole frac)	0	0	0	0.234	0.0131	0
C_{16} (mole frac)	0	0	0	0.186	0.0186	0
C_{18} (mole frac)	0	0	0	0.00464	0.00167	0
C_{20} (mole frac)	0	0	0	0.00352	0.0113	0
C_{22} (mole frac)	0	0	0	0.00190	0.0659	0
C_{24} (mole frac)	0	0	0	0	0.129	0
C_{26} (mole frac)	0	0	0	0	0.116	0
C_{28} (mole frac)	0	0	0	0	0.0930	0
C_{30} (mole frac)	0	0	0	0	0.518	0
Water (mole frac)	0.0252	1	0.00378	0.00443	0	1

Final Recommended Design

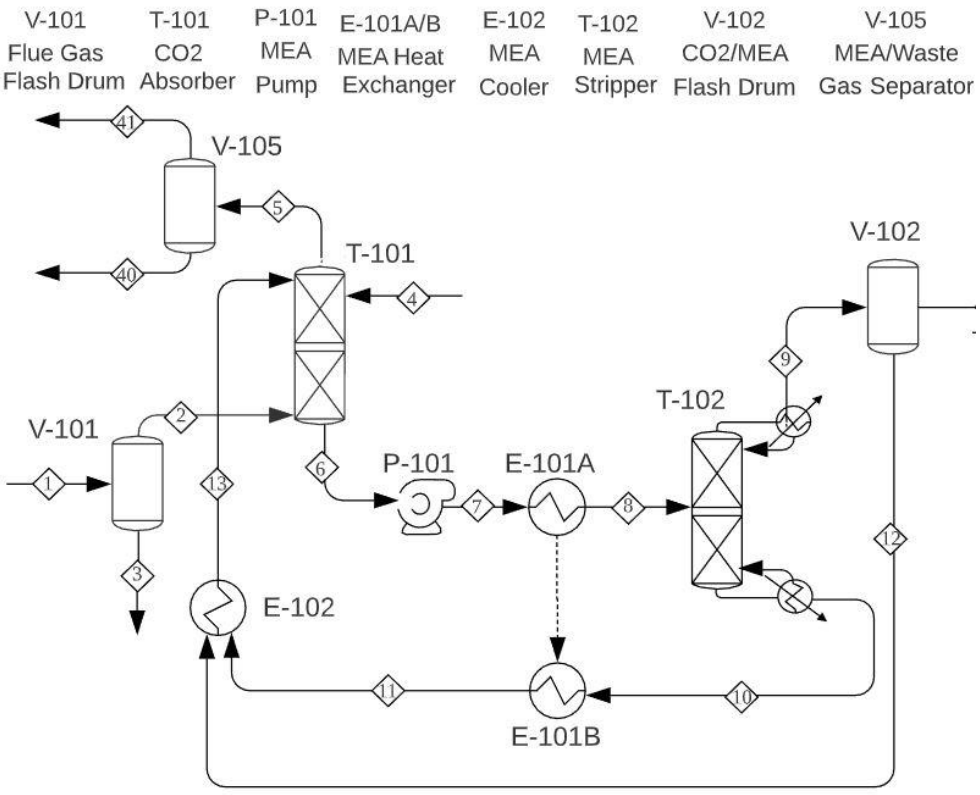

Figure 4: Process Flow Diagram: Amine Scrubbing

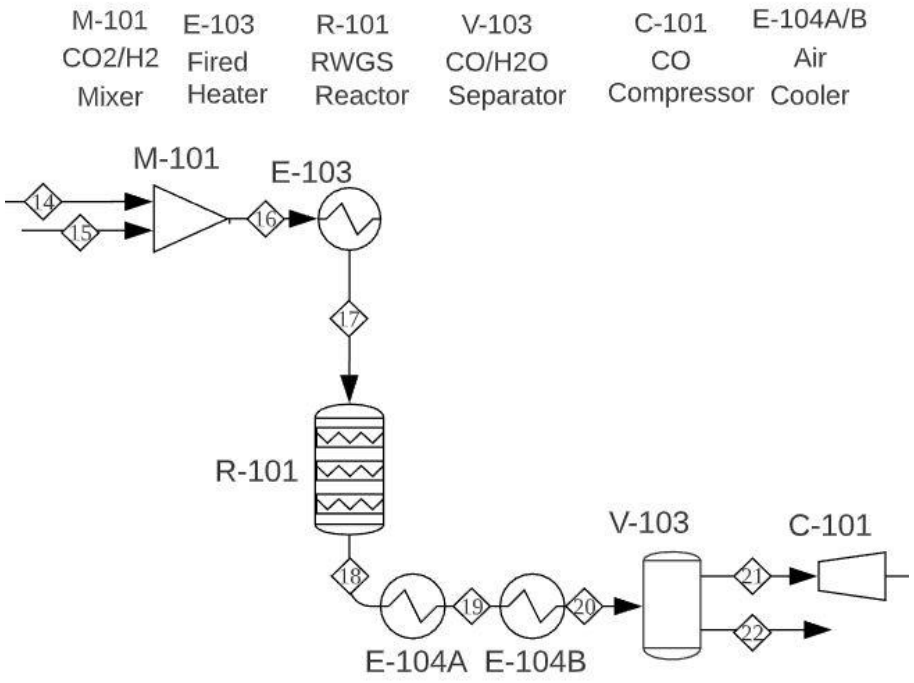

Figure 5: Process Flow Diagram - Reverse Water-Gas Shift Reaction

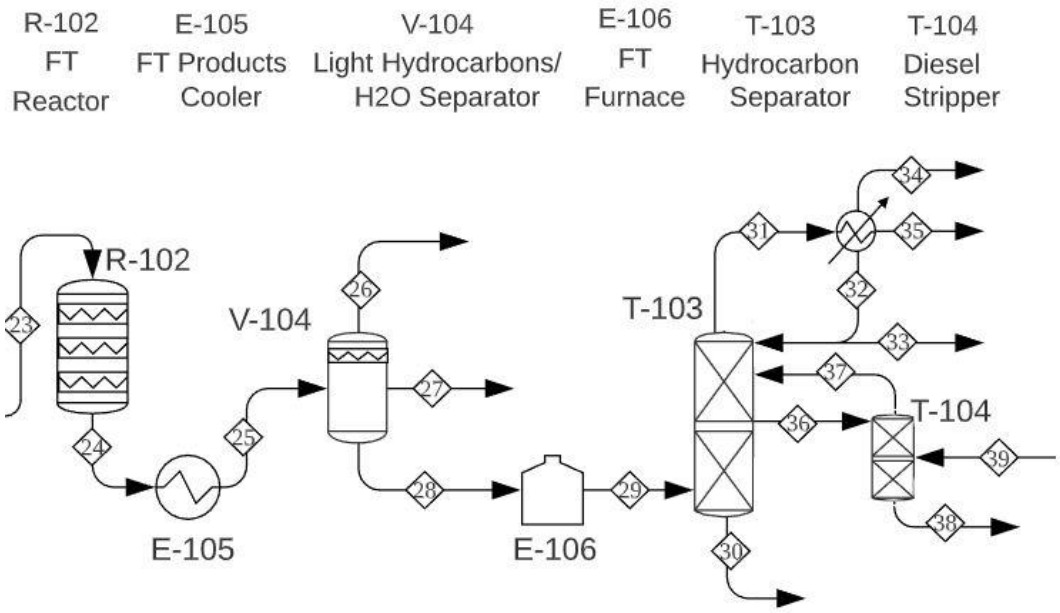

Figure 6: Process Flow Diagram - Fischer-Tropsch Reaction

Absorber and Stripper Design

The CO_2 capture process is laid out in a conventional manner with three primary components: an absorber (T-101), a stripper (T-102), and a heat exchanger (E-101) between the two. Scrubbed flue gas with negligible amounts of SO_x and NO_x enters a flash drum (V-101) to condense excess water vapor before entering the absorber. Flash drum V-101 is operated at 40℃ and 1.2 bar, and has a heat duty of -44.9 MW.

The absorber receives dry flue gas in the bottom along with a stream of MEA solvent in the top. The absorption column is packed with ½" berl saddles and has a diameter of 11.9 m and height of 10.1 m**,** giving an HEPT of 3.37. An exothermic reaction occurs between the MEA and CO_2 for absorption, and the MEA solvent rich in CO_2 exits from the bottom of the absorber and is pumped to the heat exchanger as the cold stream through pump P-101. The pump compresses the rich MEA from 1.01 bar to 5 bar at an efficiency of 0.80. The work associated with P-101 is 84 kW.

The hot stream of the heat exchanger is made up of the lean MEA bottoms product of the stripping column. The cold stream of rich MEA increases in temperature from 49 ℃ to 130 ℃ and is fed to the top of the stripper. The pressure drop of the absorption column is 0.0752 bar.

The stripper is designed as a packed column utilizing ½" berl saddles with a diameter of 13.4 m and height of 17.1 m which results in an HEPT of 2.14. It is outfitted with a condenser to allow for excess MEA in the distillate to be fed back into the column and reboiler to further remove CO_2 from the bottoms. The stripping column partial-vapor condenser is modeled as a shell and tube heat exchanger with a heat transfer area of 392 m^2. The stripping column reboiler is modeled as a U-tube reboiler with a heat transfer area of 5,700 m^2. The heat duty of the condenser is -47.7 MW, while the heat duty of the reboiler is 87.8 MW. The pressure drop of the

stripping column is 0.00814 bar. The bottoms stream of lean hot solvent is cooled from 152 ℃ to 51 ℃ through the heat exchanger.

The product stream of CO_2 enters a flash drum (V-102) to condense out water vapor and is sent to a heater before entering the water-gas-shift reactor. The flash drum is a vertical vessel with a diameter of 1.83 m and a height of 3.66 m, and is operated at 45 ℃. The heat duty of flash drum V-102 is -9.82 MW.

The condensed water from the flash drum is fed to a cooler (E-102) and recycled to the absorber with the cold lean solvent. The recycle cooler is designed as a shell and tube heat exchanger with a heat transfer area of 335 m^2 and an outlet temperature of 40 ℃. The heat duty of cooler E-102 is -5.34 MW.

Reverse Water Gas Shift Reaction

The RWGS Reactor is designed as a carbon steel packed-bed reactor with a diameter of 1 meter and a length of 3 meters, and is operated at a temperature of 400 ℃ and a pressure of 2 bar. The pressure drop across the reactor is 0.32 bar. The recommended catalyst is 0.5 weight percent Ni/SiO_2 with a particle diameter of 0.75 centimeters. E-103, the feed stream fired heater, has a heat duty of 16.9 MW and requires a heat transfer area of 337.11 m^2. E-104A, the first air cooler for the RWGS product stream, reduces the temperature from 400 ℃ to 200 °C, and has a heat duty of -9.04 MW, requiring a heat transfer area of 88.6 m^2. E104B, the second air cooler, reduces the stream's temperature from 200 °C to 40 °C, and has a heat duty of -20.6 MW, requiring a heat transfer area of 252 m^2. V-103, the RWGS products separator, is 3 meters in diameter and has a tangent to tangent height of 4 meters. This flash vessel operates at a temperature of 40 °C and a pressure of 1.01 bar, and has a heat duty of 35.6 kW. The gas product

from the reverse water-gas shift reactor (R-101) must enter the Fischer-Tropsch reactor at 220 °C and 20 barg. Therefore, the gas enters a 2 stage compressor (C-101) which requires 20.3 MW of work, running at 100% efficiency, to compress the RWGS products to 20 barg.

Fischer-Tropsch Synthesis

The pressurized gas enters, S-22, the reactor, R-102, which operates at 220 °C and 20 barg in order for the completion of the Fischer-Tropsch reaction. The reactor is a shell-and-tube reactor with room temperature boiler water (25 °C) running through the shell side. It is first compressed to 10 barg before flowing through the reactor to absorb the 77.1 MW of heat produced by R-102 which has a heat transfer area of 946.6 m^2. The heat from the reactor generates 400 metric tons/hr of 10 barg saturated steam. The reaction occurs in the tubes using a cobalt catalyst. The reaction results in approximately 95% (mole basis) conversion of the carbon monoxide from the RWGS reaction.

The products of the Fischer-Tropsch reactor leave the reactor through S-23 and flow into a heat exchanger, E-105, which cools them to 60 °C. Cooling water at 25 °C is fed to the heat exchanger which has a heat transfer area of 3,860 m^2. They are then entered into a flash drum, V-104, which separates water and a small fraction of heavier hydrocarbons, S-26, from the mid-weight hydrocarbons, S-27, and some of the lighter components, S-25, by dropping the pressure to 3.0 barg. The mid-weight hydrocarbon stream is fed to a furnace, E-106, which heats them up to 360 °C and drops the pressure to 1.7 bar. The dirty water stream (S-26) exiting the drum will be sent to a treatment plant because of the significant amount of hydrocarbons it contains. The vapor stream (S-25) that exits the flash drum will be burnt for fuel.

The components are fed to a distillation column, T-103, to be separated into lighter components and gasoline (S-34), diesel (S-39), wax (S-29), free water (S-36), and non-condensables (S-35). The distillation column utilizes the furnace (E-106) as a reboiler and has a partial condenser that runs at 30 °C using the 25 °C cooling water. The reflux ratio of the column is 10 (mole basis) and the distillate rate is 18 kmol/hr. The column has 20 stages, is 14 meters tall, and has a diameter of 1.79 m. The spacing between the bubble cap trays is 0.609 m. The pressure drop within the column is 0.085 bar. The feed stream is fed through the furnace on stage 20. The vapor distillate is removed from the column through S-35. Water is removed through S-36. Gasoline and lighter condensable components are removed through S-34. The wax components are removed through S-29 as the bottoms product. A side stream is taken from the column at stage 15 through S-37 and run through a stripper, T-104. The product of this column is S-39, the diesel fuel, and the remaining fuel is cycled back into the distillation column at stage 13. T-104 contains 3 theoretical stages and is packed with 0.5-inch berl saddles. It is reboiled using 15 barg steam flowing at 10 kmol/hr via S-40. The diesel stream contains mostly C_{10} through C_{16} components and a boiling point of around 230 °C.

Economic Analysis

Process Equipment Costs

The following equipment costs were calculated using CAPCOST based on a CEPCI value of 596.1 (Chemical Engineering, 2020).

Table 10: Amine Scrubbing Equipment Costs

Equipment Name	Base Cost (USD)
V-101	379,400
T-101	3,149,300
P-101	20,700
E-101A/B	237,800
E-102	66,600
T-102	7,815,100
V-102	27,300
V-105	288,000
Total	11,984,200

Table 11: Reverse Water-Gas Shift Equipment Costs

Equipment Name	Base Cost (USD)
M-101	32,900
E-103	1,650,000
R-101	10,800
V-103	48,200
C-101	6,160,000
E-104A/B	186,500
Total	8,088,400

Table 12: Fischer-Tropsch Equipment Costs

Equipment Name	Base Cost (USD)
R-102	26,400
E-105	142,700
V-104	23,000
E-106	1,212,000
T-103	365,800
T-104	18,300
Total	1,788,200

Capital Cost

The Lang Factor method was used to determine the total plant cost, including each piece of equipment listed in Tables 10-12, which corresponds to the following equation:

$$Plant\ Cost = F_{Lang}\ x\ \sum \quad Purchased\ Equipment\ Costs \tag{27}$$

According to Turton, for a fluid processing plant, F_{Lang} is 4.74. Multiplying this value by the total purchased equipment costs results in a capital cost of $103,620,192. The capital cost additionally includes the catalysts for both the RWGS and Fischer-Tropsch reactions, which only need to be purchased at the beginning of operations. The RWGS reaction requires 6.83 metric tons of Ni/SiO_2 catalyst, which costs $132.53 per kg. Thus, the total catalyst cost is $905,180. The Ni/SiO_2 particles can be regenerated through treatment with air (Wagner, 2009). The Fischer-Tropsch reaction requires a cobalt-silica catalyst known as SBA-15, which costs $12.00/kg. A mass of 54.8 metric tons is needed to operate the reactor, resulting in an overall cost of $657,710. Although wax buildup will occur over time, the catalyst can be reused by using either magnets or a settler to remove the heavy hydrocarbon components from the catalyst particles. Thus, this is only an up-front cost. This brings the total capital cost to $105,183,082.

Operating Costs

Raw Materials

In order to obtain a purified CO_2 product through the amine scrubbing portion of the process, 41.4 metric tons of MEA is required per year. The cost of this solvent is $2.19/kg, resulting in a total cost of $90,670 per year. In addition, this step requires 9.47 million ft^3 of water per year at a cost of $2.60 per 100 ft^3, leading to a total of $246,200 per year.

Hydrogen gas is required to fuel the RWGS reaction. The first, more environmentally conscious option is to purchase hydrogen that has been produced through solar photovoltaic electrolysis. This hydrogen costs $3.26 per gallon of gasoline equivalent (GGE), and according to the U.S. Department of Energy (2020), the conversion factor between kilograms of H_2 and GGE is 1.019. Thus, dividing $3.26 by this factor results in a cost of $3.20 per kilogram of H_2. Since the RWGS reactor requires 7.73 metric tons H_2 per hour, the total cost would be $184 million per year. The second option is to source hydrogen that has been produced through the steam reforming of methane, which costs only $1.25 per kg. This results in a cost of $9,659 per hour, or $71.9 million per year, reducing the cost significantly in comparison to electrolysis. The downside of this alternative is the additional production of CO_2 gas, which will be discussed in the Health, Safety, and Environmental Concerns section of the report.

If no mechanism is used for removing wax from the catalyst, the cobalt catalyst should be replaced every 2-3 years, adding an additional $263,084 per year on average.

Labor

The cost of operating labor is calculated using the following equations from Turton:

$$N_{OL} = (6.29 + 31.7P^2 + 0.23N_{np})^{0.5}$$

(28)

$$N_{np} = \sum \quad Equipment\ (compressors, towers, reactors, heaters, exchangers) \quad (29)$$

Where N_{OL} represents the number of operators per shift, and P represents the number of processing steps involving the handling of particulate solids, such as distribution and transportation, size control of particulates, and removal of particulates. N_{np} represents the number of nonparticulate processing steps such as heating and cooling, reactions, mixing, and compression. Many processes have a P value of 0 (Turton, 2018). The calculation for N_{np} should not be used for processes with greater than two solid handling steps. The results of equation 28 were multiplied by 5 to determine the plant's full staffing requirements. Based on this estimate, the amine scrubbing section of the plant requires 15 operators, and 14 operators are needed for both the RWGS and Fischer-Tropsch equipment, resulting in a total of 43 operators. According to the Bureau of Labor Statistics, on average, operators are paid $31.94 per hour (2018). Each operator typically works five 8-hour shifts a week for 49 weeks per year. This results in a total yearly salary of $62,600. In addition, one engineer must be hired for each of the three primary sections of the plant, each with a salary of $100,000 per year, and a plant manager is also required, with a salary of $150,000 per year. It is estimated that employee benefits cost 1.25-1.4 times their salary per individual. Using the upper end of this estimate results in a total labor cost of $4,398,520 per year.

Utilities

The average cost of electrical power in California is estimated to be $0.167/kWh (CalChamber, 2019). This was used as a basis for all utility cost calculations, assuming 7446

hours of operation per year. The costs are broken down for each section of the process in Table 13 below. Electricity must be supplied to the separation equipment at a rate of 74.7 kW. This leads to an annual electricity cost of $92,900. For E-103, a fired heater with a heat duty of 16.9 MW or -67.60 GJ, natural gas will be required at a cost of $3.16/GJ. Assuming a furnace efficiency of 90%, this results in a total cost of $1,591,000 per year. For E-106, another fired heater operating at 90% efficiency, with a heat duty of 3.69 MW, the annual cost will be $346,314.

Based on the cost of electricity, cooling water costs $0.775 per GJ. Cooling water must be supplied to the separation equipment to satisfy a combined heat duty of -0.108 GJ/s for the two cooling flash drums V-101 and V-102, the lean recycle cooler E-102 and the condenser of the stripping column T-102. The total duty of the CO_2 separations equipment that requires cooling water is 1,840 GJ, which leads to an annual cost of $10,613,000. For the RWGS equipment, E-104A, which has a heat duty of -9.04 MW, or -32.54 GJ per hour, requires $187,800 of cooling water per year. E-104B, has a heat duty of -20.6 MW, or -74.16 GJ per hour, resulting in an annual cooling water cost of $427,951. R-102, which has a heat duty of -77.1 MW, has an annual cost of $1,601,712. E-105, used to cool the Fischer-Tropsch product stream, has a heat duty of -18.0 MW, has an annual cost of $373,938 for cooling water. The condenser in T-103, which has a heat duty of -3.42 MW, has a cost of $71,048 per year for cooling water.

The price of wastewater treatment in California is $4.24 per thousand gallons for non-residential facilities (Cooley and Phurisamban, 2016). Stream 3, the wastewater stream discharged from the separation equipment, discharges 11.2 gallons of water per hour, resulting in an annual cost of $350 for treatment. Stream 20, the wastewater product from the RWGS

reaction, has a flow rate of 6,400 gallons per hour, requiring a cost of $202,054 per year. The wastewater stream, stream 26, from the Fischer-Tropsch process has a flow rate of 9,080 gallons per hour and will cost $288,612 per year.

The separation equipment requires a total of 524 klb/h steam at 100 psi to satisfy the stripping column reboiler heat duty of 87.6 MW. Steam at a pressure of 10 barg is required to maintain the temperature of R-101 throughout the RWGS reaction. R-101 has a heat duty of 13.1 MW, or 47.16 GJ. The steam is estimated to cost $6.68/GJ, resulting in a total cost of $2,345,704 per year. The heat that is removed from the RWGS process stream by E-104A can be used to produce steam. Since the heat duty of E-104A is 32.54 GJ per hour, this results in a reduction in steam costs of $1,618,516 per year. The annual cost of the steam entering T-104 is $117,609, but this cost can be eliminated by using the steam produced by E-104A. The amount of steam produced by R-102 is worth $14.4 million in 10 barg steam per year, which covers the steam requirements for the upstream separations process. The total cost of utilities for the overall process is summarized below in Table 13.

Table 13: Total Utility Costs

Utility	Cost Per Year (USD)			
	Separations	RWGS	Fischer-Tropsch	Total
Electricity	92,900	0	0	92,900
Natural Gas	0	1,591,000	346,314	1,937,314
Cooling Water	10,613,000	615,751	2,046,698	13,275,449
Wastewater	350	202,054	288,612	491,016
Steam	0	2,345,704	0	2,345,704
Total	10,706,250	4,754,509	2,681,624	18,142,383

Carbon Credit

California's industrial sector operates under the fourth-largest carbon cap-and-trade program in the world with the intention of lowering greenhouse gas emissions. This system applies to fuel distributors, large industrial plants, and large electric power plants that emit at least 25,000 tons of carbon dioxide equivalent per year or more (Center for Climate and Energy Solutions, n.d.). Each allowance represents one ton of CO_2 emitted.

Calpine is an investor-owned utility, so the company must sell free allowances and redistribute the funds to customers. Any needed allowances must be purchased at auction or via trade (Center for Climate and Energy Solutions, n.d.). The current price minimum for auction is $15.76 per allowance, increasing from $10.00 in 2012. This price will increase 5% annually over inflation until the price maximum per allowance is reached at $40 and more allowances will be available for sale. The E-Diesel produced by this process is considered carbon-neutral in a legal sense, according to the California Air Resources Board (CARB). The Pastoria Energy Facility will gain carbon credits for the CO_2 captured even though it will be converted into fuel, as confirmed by Anil Prabhu, Ph. D. who manages the Fuels Evaluation Section of the Transportation Fuels Branch of CARB. Natural gas furnaces emit 73.3 thousand metric tons of CO_2 annually, and 35.3 thousand metric tons of carbon emissions are produced from burning wax generated by the Fischer-Tropsch portion of the process. Taking this into consideration, the final revenue distributed to customer savings through carbon credits is $5.02 million per year.

Revenue

The final product of the overall process is diesel fuel, which exits the Fischer-Tropsch section of the plant at 4.50 metric tons per hour. Thus, the plant produces 33.5 million kg of

diesel per year. The current average price of diesel fuel is $2.86 per gallon, bringing in a total yearly revenue of $30.5 million per year (U.S. Energy Information Administration, 2020).

Alternate Design Scenario

Due to the high cost of operating the RWGS and Fischer-Tropsch equipment, an alternative solution would be storing the CO_2 in underground geological formations rather than producing diesel fuel. The estimated cost of transportation and storage through deep well injection is $15 per ton of CO_2 (Friedmann et al., 2006). Since the separation process removes 57.4 metric tons of CO_2 per hour from the stack, the overall cost of transportation and storage would be $6,411,006 per year.

Removing the RWGS and Fischer-Tropsch equipment from the process lowers the total equipment cost to $56,805,108, with a yearly utility cost of $13,196,015. This alternate scenario would also reduce the number of workers to 15 operators, in addition to one engineer and one manager, bringing the cost of labor and benefits down to $1,664,600 per year. Additionally, the minimum customer savings associated with the reduction of 427 thousand metric tons CO_2 emissions annually at the Pastoria Energy Facility due to carbon credit allowances add up to $6.74 million per year.

Cash Flow Analysis

Three scenarios have been evaluated for the project's overall cash flow. The first, represented by Table 12, is modeled based on purchasing hydrogen for the RWGS reaction through solar photovoltaic electrolysis. The second, shown in Table 13, is the scenario in which the hydrogen is produced through the steam reforming of methane. The final scenario,

represented by Table 14, is the case in which the CO_2 is transported and stored through deep well injection, eliminating the production of diesel fuel.

Table 14: Electrolysis Scenario Cash Flow

Year	0 - 0.5	0.5 - 1	2	3	4	5
Capital Cost (USD)	105,183,082	0	0	0	0	0
Utilities (USD)	9,079,191	9,079,191	18,142,383	18,142,383	18,142,383	18,142,383
Raw Materials (USD)	92,249,977	92,168,435	184,336,870	184,599,954	184,336,870	184,336,870
Labor (USD)	2,199,260	4,398,520	4,398,520	4,398,520	4,398,520	4,398,520
Revenue (USD)	9,682,648	19,365,296	38,730,592	38,730,592	38,730,592	38,730,592
Carbon Credit (USD)	2,510,000	2,510,000	5,020,000	5,020,000	5,020,000	5,020,000
Net Flow (USD)	-196,518,862	-83,770,850	-163,127,181	-163,390,265	-163,127,181	-163,127,181

Table 15: Methane Reforming Scenario Cash Flow

Year	0-0.5	0.5-1	2	3	4	5
Capital Cost (USD)	105,183,082	0	0	0	0	0
Utilities (USD)	9,019,425	9,019,425	18,038,849	18,038,849	18,038,849	18,038,849
Raw Materials (USD)	36,249,977	36,118,435	72,236,870	72,499,954	72,236,870	72,236,870
Labor (USD)	2,199,260	2,199,260	4,398,520	4,398,520	4,398,520	4,398,520
Revenue (USD)	9,682,648	19,365,296	38,730,592	38,730,592	38,730,592	38,730,592
Carbon Credit (USD)	2,510,000	2,510,000	5,020,000	5,020,000	5,020,000	5,020,000
Net Flow (USD)	-140,459,096	-25,461,824	-50,923,647	-51,186,731	-50,923,647	-50,923,647

Table 16: CO_2 Storage Scenario Cash Flow

Year	0-0.5	0.5-1	2	3
Capital Cost (USD)	56,805,108	0	0	0
Utilities (USD)	13,196,015	13,196,015	26,392,029	26,392,029
Raw Materials (USD)	168,435	168,435	336,870	336,870
Labor (USD)	832,300	832,300	1,664,600	1,664,600
Transportation & Storage (USD)	3,205,503	3,205,503	6,411,006	6,411,006
Carbon Credit (USD)	3,370,000	3,370,000	6,740,000	6,740,000
Net Flow (USD)	-70,837,361	-14,032,253	-28,064,505	-28,064,505

This net loss would require the 750 MW electric Pastoria Energy facility to increase the price of electricity sold by $0.0060/kWh over the 10-year span immediately following the beginning of the project in order to account for the losses during this span, which include capital costs. After the losses from capital costs have been recouped by Year 10, the price of electricity would need to increase by $0.0050/kWh for each year following Year 10. This is a percent increase of 3.6% for 10 years and 3.0% after from the average cost of electricity of $0.167 in California .

Health, Safety and Environmental Considerations

Overall Carbon Emission Analysis

The purpose of this process is to reduce carbon emissions, and each of the three scenarios outlined above has a different impact on the amount of carbon emitted to the atmosphere. The total amount of CO_2 removed from the stack gas through amine scrubbing is 55.6 metric tons/hr.

If the methane necessary to provide H_2 to the fuel-making process is produced through electrolysis, a carbon-neutral process, the only extra emissions from this process come from operation of equipment. CO_2 release generated through the implementation of this process was calculated based on on-site emissions from natural gas furnaces and wax and off gases. According to the Environmental Protection Agency's (EPA) eGRID emission factors published in 2020, an average of 0.430 kg CO_2 emissions resulted per kWh of energy consumption (U.S. EPA, 2020). Natural gas furnaces will release 73.3 thousand metric tons of CO_2 annually. Burning wax generated through the Fischer-Tropsch process releases 35.3 thousand metric tons of carbon emissions.

The main differentiation between sequestration and generation of fuel is the excess CO_2 released by consumers when the e-diesel is burned, and reduced energy requirements from discluding RWGS and Fischer-Tropsch equipment. 22.38 lbs of CO_2 are produced per gallon of diesel fuel burned (Carbon Dioxide Emissions Coefficients, 2016), and with the rate of diesel production at 5.68 metric tons/hr, the total amount of CO_2 removed from the atmosphere for this scenario amounts to 37.2 metric tons/hr.

If the more cost-effective H_2 production method of methane reforming is utilized for this process, the emissions from that process must be considered in addition to those that result from the burning of diesel fuel. Given that methane reforming required for this process would emit

958.33 kmol/hr, the CO_2 removed through amine scrubbing would be offset by the diesel fuel and methane reforming emissions, resulting in 4.98 metric tons/hr being put into the atmosphere.

If fuel production is not pursued in this process and all of the removed CO_2 is instead placed in underground wells, 55.6 metric tons/hr of CO_2 would be removed from the atmosphere.

Overall HSE

As with all major new projects at industrial facilities, a comprehensive safety and health program for both construction and operation will be implemented including an injury and illness prevention program, exposure monitoring program, fire protection and prevention plan, personal protective equipment program, emergency response plan, and other general safety measures. This equipment will be installed proceeding already existing environmental controls that will remain in operation. This facility is required to meet emissions regulation standards for NOx, SO_2, volatile organic compounds (VOC), O_2, particulate matter (PM), carbon dioxide, methane, and carbon monoxide (San Joaquin Valley Air Pollution Control District, 2016). Continuous emissions monitors (CEMs) are in place ensuring compliance; therefore, limited environmental controls are necessary for the retrofitted system and will be addressed in the following equipment-specific sections.

Mitigation techniques in the case of a disaster include response, isolation, plant layout, and personal protective equipment (PPE). A contingency plan will remain in place utilizing the plant's usual emergency response measures in the case of an emergency, including on-site and local fire protection services. If necessary, the Kern County Fire Department (KCFD) Mettler Station No. 55 will provide fire protection and emergency response, and has a typical response time of approximately 6 minutes. This station is located only 7 miles away, and the two next

nearest emergency response stations are Lebec Station 56 and Arvin Station 54, with response times of 14 and 30 minutes respectively (California Energy Commission, 2006). CO_2 fire protection systems will be necessary to implement throughout the system. HazMat response is sourced from Landco Station 66, which is located about 30 miles north of the site and has a response time of approximately 30 minutes (California Energy Commission, 2006). The westmost stack, #1 in Figure 5 below, is chosen for retrofit because its location is surrounded by the least density of equipment, and is most easily accessible in the case of an emergency.

Figure 5: Aerial view of the Pastoria Energy Facility showing each stack.

Potential failures common to the entirety of equipment in this process include external events, structural failure, maintenance faults, human error, and impact. Human error,

maintenance faults, structural failure, and impacts can be controlled by implementation of alarms for unsafe operating conditions, control systems, effective training, permits to work, leak detection, and inspection.

External event failure includes the possibility of lightning strikes and equipment damage due to other extreme weather events including hurricanes and tornadoes. Controls put into place to prevent this kind of damage include wind loading protection, lightning protection, and relief systems. Lightning is a potential ignition source and can lead to electrical surges that may result in catastrophic failures. The National Fire Protection Association (NFPA) standard for installation of lightning protection systems, Standard 780, states that facilities that generate electric power as their primary purpose are excluded from this standard due to electrical utilities having their own standards covering the protection of facilities and equipment (NFPA, 2020).

Carbon Separation Equipment

The United Kingdom Health and Safety Executive identifies the failure modes associated with absorption and stripping columns as: corrosion, design fault, maintenance faults, overheating, external events, overpressurization, fire or explosions, structural failure, vibration, human error, impact, wrong or defective equipment, and impurities (Health and Safety Executive, n.d.). Assuming the team is diligent enough to prevent design faults and utilization of incorrect or defective equipment upon implementation of this system through inspection and detection measures, eleven potential failure modes are still of concern, five of which were addressed above under the *Overall HSE* subsection.

Degradation of MEA can lead to issues such as excessive corrosion, foaming, reduced absorption capacity, viscosity changes, and amine loss. There is no difference in the degree of

degradation between MEA in stainless steel or glass. Increased temperature tends to lead to higher rates of MEA degradation (Eide-Haugmo, et al., 2011). Overall, MEA is non-corrosive in the presence of CO_2 and at overstripped conditions, but severe corrosion can occur at lean, hot conditions (Fischer, 2017). Stainless steel has a passivating chromium oxide film that requires relatively oxidizing conditions to remain stable, so failures are often found to occur in the reboiler and stripper sump due to oxygen-depleted conditions (Fischer, 2017). Control measures preventing failure from corrosion include monitoring, inspection, and leak detection.

Overheating of absorption and stripping equipment can be prevented by completing thorough maintenance procedure and ensuring the reliability of utilities. Design and operating procedures must meet applicable OSHA regulations and be followed strictly. Necessary controls for such an event include alarms, back-up cooling, response training, trips, and ventilation systems (Health and Safety Executive, n.d.). The emergency response plan, isolation of equipment, proper plant layout, and use of proper PPE will ensure that, if disaster were to occur despite the best prevention and control, negative repercussions would be limited to the fullest extent. Fires and explosions are controlled and prevented similarly to overheating, but require active fire protection and response which was addressed in the prior section.

Overpressurization is a very limited concern in this process due to the near-atmospheric pressures at which the equipment operates. To ensure that pressure does not build unknowingly, alarms, relief systems, training, trips, and ventilation systems will be included for major equipment. Vibration is also controlled through proper use of design codes and failures due to vibrations are controlled through leak detection, proper maintenance and training, and regular inspection. Impurities causing major accidents are of limited concern in this process as well, but alarms and relief systems will also be included to ensure purity of operating streams. Proper

response, PPE, and containment are measures to mitigate negative effects from any failure incidents caused by overpressurization, vibration, or stream impurities.

The carbon capture segment of the proposed process is an environmental control in and of itself, and is implemented following existing environmental controls that maintain compliance at the Pastoria Energy Facility. That being said, the most relevant concern in an environmental sense is the disposal of MEA waste. The potential options for this waste include reuse, recycling, treatment, and final disposal. MEA waste can be treated through a series of biological processes such as time spent in an oxidation ditch, use of a trickling filter, and Complete-Mix Activated Sludge (CMAS) treatment. Secondary biological treatment costs approximately \$0.017 - \$0.02 per ton of CO_2 removed. Destruction of MEA waste could serve as a means to generate energy through incineration on site for a cost of approximately \$0.031 per ton of CO_2 captured (Nurrokhmah et al., 2013). The most effective solution when taking both sustainability and economics into consideration, though, is reuse for NO_x scrubbing, since the waste itself can be sold to generate a small revenue and prevent further emissions through incineration.

Reverse Water-Gas Shift Reaction

If the hydrogen gas that is required for the RWGS reaction is sourced through the steam reforming of methane, the additional CO_2 emitted by this process must be taken into account. For every four moles of hydrogen produced, one mole of carbon dioxide is produced, according to the following reaction:

$$CH_4 + 2H_2O \leftrightarrow CO_2 + 4H_2 \quad (30)$$

Since the reaction requires a feed of 3.83 x 10^3 kmol H_2 per hour, the process would produce 958.33 kmol CO_2 per hour, or 42.2 metric tons. This factor must be considered when evaluating carbon credit earned through reducing the Pastoria Energy Facility's CO_2 emissions.

In addition, since the RWGS reactor is operated at a high temperature of 400 °C, it is crucial for operators who are in proximity of this equipment wear proper heat protective PPE, and limit contact to the maximum possible extent.

Fischer-Tropsch Reaction

The Fischer -Tropsch reaction produces a significant amount of wastewater that must be transported to a treatment facility. Contamination by heavy hydrocarbons, including paraffins, means that this water cannot be disposed of without treatment.

Because the process includes a fired heater, it is possible that ash produced will escape into the atmosphere. Proper precautions should be taken to ensure that ash is collected and disposed of in a landfill. In addition, because of the presence of high-temperature equipment, like the fired heater and the Fischer-Tropsch reactor, employees who must come into contact with the equipment should wear the proper PPE. Relatively high pressure steam is present in almost every unit operation within this section of the plant. Therefore, employees should adhere to proper safety regulations and also wear the proper PPE.

Cobalt catalyst is manufactured from mined cobalt. Mines pose an environmental hazard, causing destruction to the surrounding ecosystem. Increased noise from drilling, flooding, erosion, and heavy-metal leaching are only a few of the negative consequences of mining.

The wax produced in the Fischer-Tropsch process can be burned in a furnace to produce heat. This process produces carbon dioxide based on the reaction shown below if burned to completion:

$$C_{27.5}H_{57} + 41.25O_2 \rightarrow 27.5\,CO_2 + 27.5\,H_2O \quad (31)$$

Burning all of the wax produced by the Fischer-Tropsch process would result in 10.8 kmol per hour of carbon dioxide being produced, or 474 kg per hour.

The purpose of this Capstone is to reduce carbon dioxide emissions of Pastoria Energy Facility. The diesel fuel, once sold and used, will produce carbon dioxide. Presumably, the vehicle using it will not have a carbon capture system so it will be released into the atmosphere where it will be more difficult to capture than if it were more concentrated.

Conclusion and Recommendations

Based on the research conducted for this carbon capture and utilization process, it is not economically feasible at this time to retrofit an amine scrubbing and diesel generation system to the Pastoria Energy Facility. This is largely due to the difference in cost of diesel fuel and clean H_2 needed to complete the process. If electrolytic H_2 is purchased to reduce carbon emissions, the project runs at a net loss of nearly $3 billion per year to remove 37.2 metric tons/hr of CO_2 from the atmosphere. If H_2 is purchased from methane reforming, the project runs at a less severe net loss of $56 million per year, but also introduces 4.98 metric tons/hr of CO_2 into the atmosphere, defeating the purpose of the project entirely.

The alternative solution of eliminating the diesel fuel production steps of this CCUS process and instead storing the captured CO_2 in underground wells is far more economically feasible. While this project would generate no income, it would operate at a net loss of a far more manageable $2 million per year after initial capital costs of $55 million. This would require the Pastoria Energy facility to increase their electricity prices by 0.83% over the 10 years following the project, and 0.21% after that, assuming the average electricity cost of $0.167/kWh in California.

As a result, it is recommended that the Pastoria Energy Facility or other similar natural gas power plants pursue a CCS system that involves storing captured carbon in wells, as it is believed that consumers would be willing to increase their electricity costs by 0.83% or 0.21% to purchase more environmentally friendly energy. This would leave the Pastoria Energy Facility at a breakeven point financially, but would drastically reduce the plant's carbon footprint.

Acknowledgments

The team would like to extend our gratitude to Professor Eric Anderson for his contributions to our success in completing this capstone design project. The modeling and simulations would surely not have converged effectively without the guidance supplied from his vast knowledge of ASPEN PLUS modeling, and other means of modeling chemical processes. The wisdom provided from his background in industrial settings was an invaluable asset

Nomenclature

a_i - Activity of species i

A - Heat transfer area

α - Probability of chain growth

d_p - Particle diameter

D - Diameter

ε - Catalyst void fraction

F - Molar flow rate

k_j - Rate constant of reaction j

K_i - Chemical equilibrium constant of species i

L - Length

n - Number of carbon atoms in a hydrocarbon

N_{np} - Number of nonparticulate processing steps

N_{OL} - Number of plant operators per shift

μ - Liquid viscosity

p - Pressure

P - Number of processing steps

Q - Rate of heat transfer

r_i - Rate of reaction j

X - Fractional conversion

T_i - Temperature of stream i

ΔT_{lm} - Log mean temperature difference

u - Velocity

U - Overall heat transfer coefficient

V - Volume

W - Catalyst weight

W_n - Weight fraction of hydrocarbon with n carbon atoms

Appendix

Sample Calculations

RWGS Reactor Pressure Drop Calculation:

$$\Delta p = L\left(\frac{150\mu(1-\varepsilon)^2\, u_0}{\varepsilon^3 {d_p}^2} + \frac{1.75(1-\varepsilon)\rho {u_0}^2}{\varepsilon^3 d_p}\right)$$

$$= (1\ m)\left(\frac{150(2.64\ x\ 10^{-5}\ \frac{Ns}{m^2})(1-0.5)^2(0.023\ \frac{m}{s})}{(0.5)^3(7.5\ x\ 10^{-5})^2}\right.$$

$$\left. + \frac{1.75(1-0.5)(0.449\ \frac{kg}{m^3})(0.023\ \frac{m}{s})^2}{(0.5)^3(7.5\ x\ 10^{-5})}\right)$$

$$\Delta p = 0.32\ bar$$

E-103 Heat Transfer Area Calculation:

q_{total} = (38000 + 12000) = 50000 W/m^2

Q_{heater} = 1.69 x 10^4 kW

$A = 1.69\ x\ 10^4\ kW \times \frac{1000\ W}{1\ kW} \times 50000\ W/m^2 = 337.11\ m^2$

E-104A/B Heat Transfer Area Calculation:

U = 450-570 W/m^2; Average = 510 W/m^2

$Q_{E\text{-}104A}$ = -9.04 x 10^3 kW

$Q = UA\Delta T \rightarrow A = \frac{Q}{U\Delta T} = \frac{-9.04\ x\ 10^3\ kW \times 1000\ W/kW}{(510\ W/m^2)(200-400)} = 88.6\ m^2$

$Q_{E\text{-}104B}$ = -2.06 x 10^4 kW

$$A = \frac{Q}{U\Delta T} = \frac{-2.06\ x\ 10^4\ kW\ \times\ 1000\ W/kW}{(510\ W/m^2)(40-200)} = 252\ m^2$$

Breakeven Calculation for CCS Scenario:

x = Increase in electricity price ($/kWh)

L_0 = Total Losses Year 0 - 0.5 = $70,837,361

$L_{0.5}$ = Total Losses Year 0.5 - 1 = $14,032,253

L_{1+} = Total Losses after Year 1 = $28,064,505

E = Electric output of Pastoria Energy Facility = 750MW = 750×10^3 kW

t = Number of operational hours per year = 7446 h

Assumes 10 year breakeven point

$x = \frac{L_0+L_{0.5}+9(L_{1+})}{E*10(t)} = \frac{70,837,361 + 14,032,253 + 9(28,064,505)}{750E03 * 10(7446)} = \$0.00604/kWh$ increase

Furnace CO_2 Emissions Calculation

Cost per year of natural gas furnace operation = $1,937,314

Annual energy consumption = $1,937,314/($3.16/GJ) = 613074.05 GJ

$$613074.05\ GJ \times \frac{278\ kWh}{1\ GJ} = 170434585.9\ kWh$$

$$\frac{0.43\ kg\ CO_2}{1\ kWh} \times 170434585.9\ kWh = 73286871.94\ kg\ CO_2$$

References

Afkhamipour, M., & Mofarahi, M. (2017). Review on the mass transfer performance of CO2 absorption by amine-based solvents in low- and high-pressure absorption packed columns. *RSC Adv.*, *7*(29), 17857–17872. https://doi.org/10.1039/C7RA01352C

Anderson, E. (n.d.) Plant Design and Economics for Chemical Engineers, Fifth Edition: Appeldix E: Heuristics for Process Design. *University of Virginia.* Pages 974-981.

Audi. (2017, August 11). Audi steps up research into synthetic fuels. Retrieved from https://www.audi-mediacenter.com/en/press-releases/audi-steps-up-research-into-synthetic-fuels-9546

U.S. Bureau of Labor Statistics. (2018). Occupational Employment Statistics: May 2018 National Occupational Employment Wage Estimates. *United States Department of Labor*. Retrieved from https://www.bls.gov/oes/2018/may/oes_nat.htm

California cap and trade. (2019). *Center for Climate and Energy Solutions*. Retrieved from https://www.c2es.org/content/california-cap-and-trade/

California electricity prices: No. 7 in U.S. (2019). *CalChamber*. Retrieved from https://calchamberalert.com/2019/03/29/california-electricity-prices-no-7-in-u-s/

California Energy Commission. (2006). Pastoria Energy Facility Expansion: Application for Certification (05-AFC-1). *Energy Resources Conservation and Development Commission of the State of California.* Retrieved from https://ww2.energy.ca.gov/2006publications/CEC-800-2006-006/CEC-800-2006-006-CMF.PDF

Carbon Dioxide Emissions Coefficients. (n.d.). US EIA. Retrieved April 8, 2020, from https://www.eia.gov/environment/emissions/co2_vol_mass.php

Cooley, H., and Phurisamban, R. (2016). The cost of alternative water supply and efficiency options in california. *Pacific Institute.* Retrieved from https://pacinst.org/wp-content/uploads/2016/10/PI_TheCostofAlternativeWaterSupplyEfficiencyOptionsinCA.pdf

Economic indicators. (2020). *Chemical Engineering*, *2*, 56. Retrieved from http://proxy01.its.virginia.edu/login?url=https://search.proquest.com/docview/2354854738?accountid=14678

Eide-Haugmo, I., Lepaumier, H., Einbu, A., Vernstad, K., Silva, E., Svendsen, H. (2011). Chemical stability and biodegradability of new solvents for CO_2 Capture. *Energy Procedia. 4*. 1631-1636. 10.1016/j.egypro.2011.02.034.

Engineering Pro Guides. (n.d.). Condensed Water Pump Design Guide: Quickly determine pump sizing and complete pump schedule. Retrieved from https://www.engproguides.com/condenser-water-pump-design.html

The Engineering ToolBox. (n.d.). Pumping Water - Energy Cost Calculator. Retrieved from https://www.engineeringtoolbox.com/water-pumping-costs-d_1527.html

Evans, J. (2012). Pump Efficiency - What is Efficiency? *Pumps and Sysetms.* Retrieved from https://www.pumpsandsystems.com/pump-efficiency-what-efficiency

Fischer, K.B., Daga, A., Hatchell, D., Rochelle, G.T. (2017). MEA and Piperazine Corrosion of Carbon Steel and Stainless Steel. *Energy Procedia*, Volume 114, Pages 1751-1764, ISSN 1876-6102, https://doi.org/10.1016/j.egypro.2017.03.1303.

Friedmann, S. J. et al. (2006). The low cost of geological assessment for underground CO_2 storage: Policy and economic implications. *Energy Conversion and Management*, *47*, 1894-1901.

Garcia, M., Knuutila, H. K., Gu, S. (2017). ASPEN PLUS simulation model for CO_2 removal with MEA: Validation of desorption model with experimental data. *Journal of Environmental Chemical Engineering*. Volume 5, Issue 5. Pages 4693-4701, ISSN 2213-3437, https://doi.org/10.1016/j.jece.2017.08.024.

Health and Safety Executive. (n.d.). Absorption / Adsorption / Stripping columns. Retrieved from https://www.hse.gov.uk/comah/sragtech/systems1.htm#

Hikita, H., Asai, S., Ishikawa, H., Honda, M. (1997) The kinetics of reactions of carbon dioxide with monoethanolamine, diethanolamine, and triethanolamine by a rapid mixing method. In Pinset, B.R., Pearson, L., and Rouchton, F.J.W. (Eds.), Chem Eng. J., 13, (pp. 7-12). Elsevier.

Jung, J., Jeong, Y.S., Lim, Y., Lee, C.S., Han, C. (2013) Advanced CO_2 Capture Process Using MEA Scrubbing: Configuration of a Split Flow and Phase Separation Heat Exchanger. *Energy Procedia*, *Vol 37*. Pages 1778-1784, ISSN 1876-6102, https://doi.org/10.1016/j.egypro.2013.06.054.

Jungcurt, S. (2019, April 2). Global energy demand in 2018 grew at fastest pace in a decade. *IISD.* Retrieved from https://sdg.iisd.org/news/global-energy-demand-in-2018-grew-at-fastest-pace-in-a-decade

Levin, Kelly. (2018, December 5). New global CO_2 emissions numbers are in. They're not good. *World Resource Institute.* Retrieved from https://www.wri.org/blog/2018/12/new-global-co2-emissions-numbers-are-they-re-not-good

Liao, P., Wu, X., Li, Y., Wang, M., Shen, J., Lawson, A., & Xu, C. (2018, July 17). Application of piece-wise linear system identification to solvent-based post-combustion

carbon capture. *Fuel, 234*, 526-537. Retrieved from https://www.sciencedirect.com/science/article/pii/S0016236118312444

Marjollet, A. (2016, August 30). Permit to operate. *San Joaquin Valley Air Pollution Control District.* Retrieved from https://www.valleyair.org/notices/Docs/2016/08-30-16(S-1153617)/S-1153617.pdf

National Fire Protection Association. (2020). NFPA 780: Standard for the Installation of Lightning Protection Systems. Retrieved from https://www.nfpa.org/codes-and-standards/all-codes-and-standards/list-of-codes-and-standards/detail?code=780

Nurrokhman, L., Mezher, T., and Abu-Zahra, M.R.M. (12 November 2013). Evaluation of handling and reuse approaches for the waste generated from MEA-based CO_2 capture with the consideration of regulations in the UAE. *Environ. Sci. Technol.* 47, 23, 13644-13651, https://doi.org/10.1021/es4027198

Ostadi, M., Rytter, E., Hillestad, M. (2016) Evaluation of kinetic models for Fischer-Tropsch cobalt catalyst in a plug flow reactor. *Chemical Engineering Research and Design*. 114, 236-246.

Pastor-Perez, et al. CO_2 valorisation via reverse water-gas shift reaction. *Journal of CO_2 Utilization, 21*, 423-428.

Pinsent, B.R.W., Pearson, L., Roughton, F.J.W. (1956) The kinetics of combination of carbon dioxide with hydroxide ions. *Trans. Faraday Soc.* 52, 1512-1520.

Physicians, Scientists, and Engineers for Healthy Energy. (2019). California power map. *PSE*. Retrieved from https://www.psehealthyenergy.org/california-power-map/

Rochelle, G.T. (2009) Amine scrubbing for CO_2 capture. *US National Library of Medicine National Institutes of Health.* 325(5948):1652-4. doi: 10.1126/science.1176731.

San Joaquin Valley Air Pollution Control District. (2016). Final Title V Permit Renewal Evaluation. Retrieved from https://www.valleyair.org/notices/Docs/2016/08-30-16(S-1153617)/S-1153617.pdf

Schulz, H. (1999). Short history and present trends of Fischer–Tropsch synthesis. *Applied Catalysis A: General*, *186*(1-2), 3–12. doi: 10.1016/s0926-860x(99)00160-x

Smith, B., Loganathan, M. & Shantha, M. S. (2010). A review of the water gas shift reaction kinetics. *International Journal of Chemical Reactor Engineering*, *8*. Retrieved from http://citeseerx.ist.psu.edu/viewdoc/download?doi=10.1.1.463.6890&rep=rep1&type=pdf

Song, C., Pan, W., Srimat, S. T., Zheng, J., Li, Y., Wang, Y., Xu, B., Zhu, Q. (2004) Tri-reforming of Methane over Ni Catalysts for CO_2 Conversion to Syngas With Desired H2/CO Ratios Using Flue Gas of Power Plants without CO_2 Separation In S.-E. Park, J.-S. Chang and K.-W. Lee (Eds.), *Studies in Surface Science and Catalysis*. (pp. 315-322). Amsterdam, The Netherlands: Elsevier B. V. Retrieved from https://www.sciencedirect.com/science/article/pii/S0167299104802702

Spath, P. L. & Dayton D. C. (2003), Technical and economic assessment of synthetic gas to fuels and chemicals with emphasis on the potential for biomass-derived syngas. *National Renewable Energy Laboratory.*

State & alternative fuel provider fleets. (2020). *U.S. Department of Energy*. Retrieved from https://epact.energy.gov/fuel-conversion-factors

Transforming industry through CCUS. (2019). *International Energy Agency.* Retrieved from https://www.iea.org/publications/reports/TransformingIndustrythroughCCUS/

Turton, R. et al. (2018). Analysis, Synthesis, and Design of Chemical Processes (5th ed.). Upper Saddle River, New Jersey: Pearson Education International.

U.S. Environmental Protection Agency. (2020). eGRID Summary Tables 2018. Retrieved from https://www.epa.gov/sites/production/files/2020-01/documents/egrid2018_summary_tables.pdf

VTT. (2019, September 26). Complete production chain from biomass residues to Fischer-Tropsch products successfully validated. Retrieved from https://www.vttresearch.com/en/news-and-ideas/complete-production-chain-biomass-residues-fischer-tropsch-products-successfully

Wagner, J. P. (2009, August 5). Water gas shift catalysis. *Catalysis Reviews*, *51,* 325-400. Retrieved from https://www.tandfonline.com/doi/abs/10.1080/01614940903048661?journalCode=lctr20

Weekly gasoline and diesel prices. (2020). U.S. Energy Information Administration. Retrieved from https://www.eia.gov/dnav/pet/pet_pri_gnd_dcus_nus_w.htm

Wu, H. C. et al. (2015, July 1). Methanation of CO_2 and reverse water gas shift reactions on Ni/SiO_2 catalysts: The influence of particle size on selectivity and reaction pathway. *Catalysis Science & Technology*, *8,* 1606-1614. Retrieved from https://pubs.rsc.org/en/content/articlelanding/2015/cy/c5cy00667h#!divAbstract

Zhang, Y., Chen, C.C. (2013). Modeling CO_2 Absorption and Desorption by Aqueous Monoethanolamine Solution with Aspen Rate-based Model. *Energy Procedia, Vol 37*. Pages 1584-1596, ISSN 1876-6102, https://doi.org/10.1016/j.egypro.2013.06.034.